MECHANOCHEMISTRY OF SULPHIDES
From minerals to advanced nanocrystalline materials

P. Baláž[*] *and E. Dutková*

Institute of Geotechnics, Slovak Academy of Sciences, Watsonova 45, 043 53 Košice, Slovakia

At present mechanochemistry of sulphides appears to be a science with a sound theoretical foundation exhibiting a wide range effectiveness in different areas of science and technology. For traditional application mechanochemistry is of exceptional importance in extractive metallurgy of sulphidic ores where many technological processes have been developed. Metal sulphides can be also utilized in emerging nanotechnology with application as advanced luminescence, optoelectronic, magnetic and catalytic materials.

Introduction

Sulphides play an important role in extractive metallurgy as sources of non-ferrous and precious metals. Mastering the processing of sulphides as well as their new applications as advanced materials (Table 1) requires a deeper knowledge of their solid-state properties. The new methods of solid treatment are studied in order to improve their technological processing. Among them, mechanochemical routes [1] strongly influence the field of the traditional as well as advanced applications of sulphides.

It is aim of this review paper to illustrate the progress in mechanochemistry of sulphides achieved recently in Slovakia [2–18]. The selected topics will be given covering the different fields of traditional and advanced applications of sulphides.

Mechanochemical treatment of sulphidic minerals

Enhancement of gold and silver recovery

The most frequent sulphides in which precious metals are present as pyrite FeS_2, arsenopyrite $FeAsS$ and stibnite Sb_2S_3, other minerals, such as chalcopyrite $CuFeS_2$, sphalerite ZnS and galena PbS also contain small amounts of Au and Ag. The sulphidic minerals which occur in the form of sulfosalts (e.g. tetrahedrite $Cu_{12}Sb_4S_{13}$) and have content of precious metals cause considerable problems in leaching of Ag. In this case, the classical cyanide leaching does not allow leaching of more than 5–10% Ag [19].
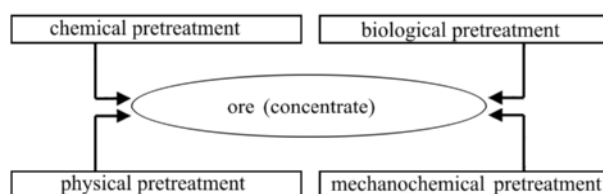

Fig. 1 The different ways of sulphidic ore (concentrate) pretreatment [2]

Some type of ore pretreatment is needed in order to improve the precious metal extraction (Fig. 1). Chemical and biological pretreatments consist of oxidizing roasting, pressure oxidation and bacteria attack. The goal of these is to disintegrate the sulphide and thus to facilitate the subsequent extraction of precious metals. Physical pretreatment consists of fine grinding of ore. If the gold encapsulated within the matrix of sulphide minerals is somewhat coarser in size, ranging from 1 to 20 microns, the liberation can be achieved by ultrafine grinding in an attritor [20]. Mechanochemical pretreatment based on the synergetic effect of mechanical activation and leaching has been verified as an effective tool for gold and silver extraction from refractory sulphidic ores [2].

We studied the acid non-cyanide leaching of silver from silver bearing tetrahedrite $Cu_{12}Sb_4S_{13}$ pretreated by mechanical activation. Thiourea, $CS(NH_2)_2$ is an attractive alternative for cyanide because of its low toxicity and higher selectivity acts according to equation

$$Ag + 3CS(NH_2)_2 + Fe^{3+} \rightarrow Ag[CS(NH_2)_2]_3^+ + Fe^{2+} \quad (1)$$

The samples of tetrahedrite mechanically activated in a planetary mill were subjected to thiourea leaching and the results are summarized in Fig. 2. The

* Author for correspondence: balaz@saske.sk

Table 1 Sulphides in traditional and advanced application

| Traditional application	Metal sulphide	Advanced application	Metal sulphide
chemical engineering		high-energy density batteries	TiS_2
Hydrodenitrogenation	Co_9S_8	solar cells	FeS_2, CuS, ZnS, CdS
Hydrodesulphurisation	MoS_2, WS_2	solar energy conversion materials	$CuInS_2$
Dehydratation	CuS, MnS, ZnS, PbS	diagnostic materials	Ag_2S
mechanical engineering		luminescence materials	ZnS, CdS: Mn, Cu, Pb
Lubricants	MoS_2	superconductors	La_2S_3, CuS
mineral processing and extractive metallurgy		intercalation compounds	TiS_2, TaS_2, NbS_2
Hydrometallurgy	ZnS, $Cu_{12}Sb_4S_{13}$	ion-selective sensors	PbS, CdS, CuS
Biohydrometallurgy	FeAsS, FeS_2	optical coatings	ZnS
Pyrometallurgy	$CuFeS_2$, PbS	photoconductors	ZnS, Ag_2S
		lasers	CdS
		light emitting diodes	CdS
		photolithographic materials	As_2S_3
		optical recordings	As_2S_3
		optical fibers	As_2S_3
		infrared detectors	PbS
		high-temperature thermistors	Cu_2S
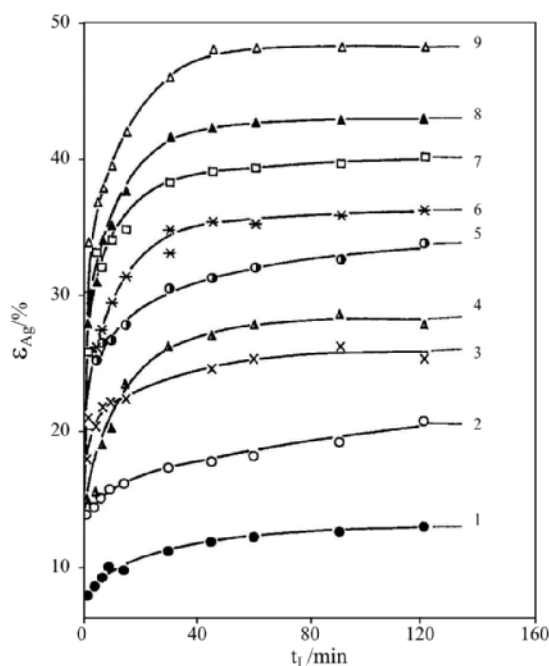
Fig. 2 Silver recovery, ε_{Ag} vs. leaching time, t_L for tetrahedrite mechanically activated in a planetary mill. Mechanical activation: 1 – 2, 2 – 5, 3 – 10, 4 – 30, 5 – 15, 6 – 20, 7 – 60, 8 – 90 and 9 – 45 min

Fig. 3 Rate constant of Ag leaching, k vs. surface/bulk disordering ratio, $S_A/(1–R)$, S_A – surface area, R – disordering of tetrahedrite structure

enhancement in recovery for the milled samples can be observed.

Figure 3 represents the quantitative relationship between the rate of thiourea leaching and surface/bulk properties of mechanically activated samples. Activati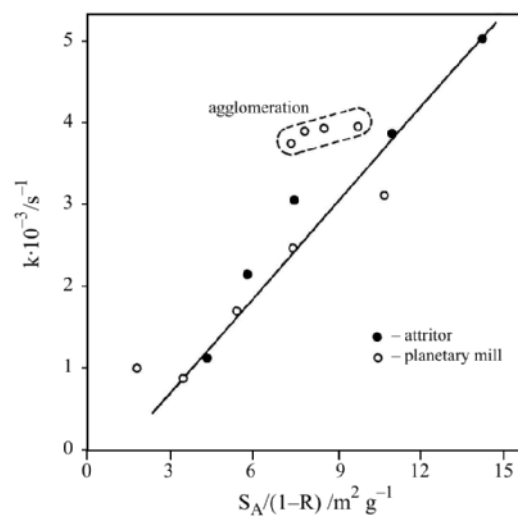on has been performed in an attritor as well as in a planetary mill. The rate constant has been correlated with the empirical coefficient $S_A/(1–R)$ which represents the surface/bulk disordering ratio for the mineral. The plot in Fig. 3 shows that the extraction of silver from tetrahedrite is a structure sensitive reaction. An equal rate of leaching can be attained by mechanical activation either in an attritor or in planetary mill (the results for samples activated in attritor are not given here). This observation is also of prognostic character because it enables us to propose
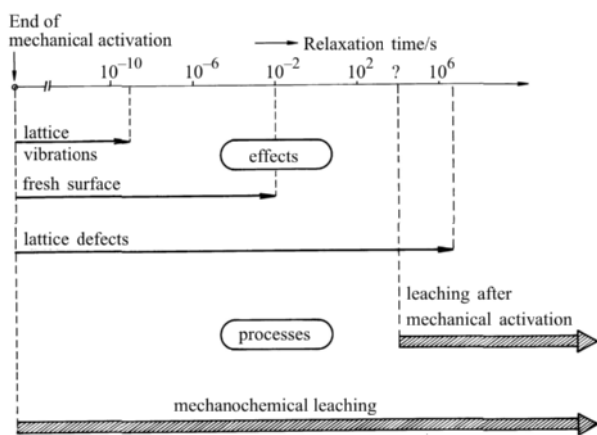
Fig. 4 The period and the duration of excitation states after termination of mechanical activation [21]

suitable grinding equipment according to the demand for fineness or reactivity of the solid substances.

Mechanochemical leaching of antimony in pilot plant unit

Mechanochemical leaching as a smart solution of hydrometallurgical problems integrates the milling and leaching operations into one common step. The synergistic effect has the important theoretical background as can be deduced from Fig. 4, which shows differences between the excitation period and the duration of excitation states. If the mechanical activation is separated from the chemical process (e.g. leaching) in time, then a number of highly excited states would have decayed before leaching. On the other hand, if the mechanical activation and leaching are integrated into a common step all the excitation states may be utilized. In addition to the improvement of grinding performance (the leaching agent works also as grinding additive) there is the possibility that a common grinding and leaching step contributes to operation at benefits and to the economy of the overall process.

The principle of mechanochemical leaching has been applied to the hydrometallurgical treatment of tetrahedrite concentrates. The reaction of refractory tetrahedrite with Na_2S as an alkaline leaching agent is described by the simplified equations

$$2Cu_3SbS_3(s)+Na_2S(l)\rightarrow 3Cu_2S(s)+2NaSbS_2(l) \quad (2)$$

$$NaSbS_2(l)+Na_2S(l)\rightarrow Na_3SbS_3 \quad (3)$$
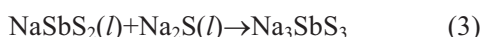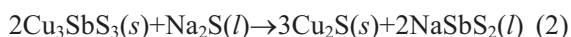
Simultaneous leaching and milling greatly intensify the whole process. The concept of mechanochemical leaching of tetrahedrites (process MELT) originally developed in the laboratory and semi-industrial attritors was further tested in a pilot plant unit in Slovakia. The flowsheet is given in Fig. 5 and con-
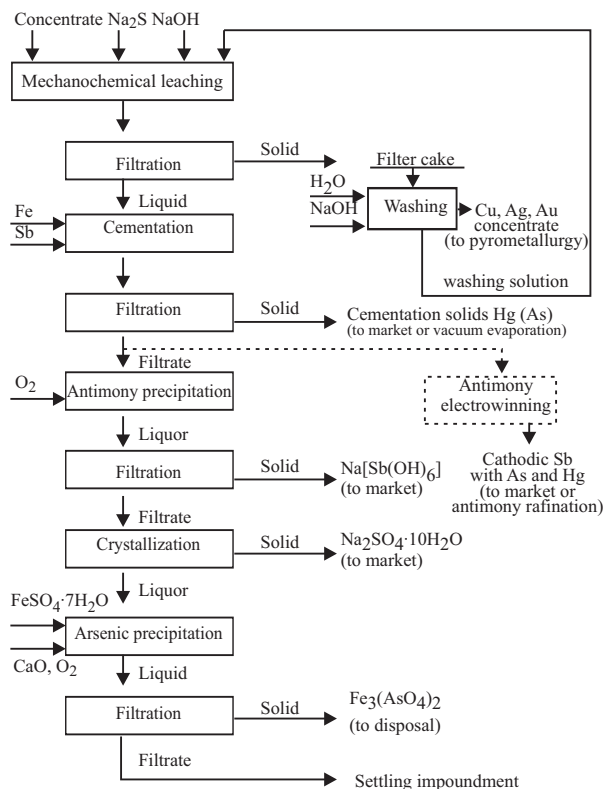

Fig. 5 Flowsheet of the MELT process

sists of primary mechanochemical leaching and the subsequent operations for production of Cu–Ag–Au concentrate, Hg(As) cementation solid, antimony electrowinning and/or $Na[Sb(OH)_6]$ synthesis as well by products processing.

The reaction kinetics is slow and high temperatures and the long leaching times are needed to obtain high recoveries [22].

Preparation of nanocrystalline metals by mechanochemical reduction of sulphides

Nanocrystalline metals have been of interest of more than 20 years and this interest is still increasing. The main cause is in their unusual properties based on the high concentration of atoms in interfacial structures and the relatively simple ways of their preparation [23–28]. High-energy milling as a way for nanomaterials synthesis has been originally developed in metallurgy as a means to prepare oxide dispersion strengthened solids [29, 30]. Later the application has been directed to the preparation of amorphous alloys, superconducting materials, rare permanent magnets, superplastic alloys and intermetallic compounds. Additionally, it has been recognized that this technique can be used to induce chemical reactions in powder mixtures at room temperature or at much lower

temperatures than normally required to synthesize pure metals [31–38].

Copper sulphide and iron system

The mechanochemical reaction between copper sulphide, Cu_2S and elemental iron is described by the equation

$$Cu_2S + Fe \rightarrow 2Cu + FeS \qquad (4)$$

The reaction is thermodynamically possible at ambient temperature, as a small but negative enthalpy change ($\Delta H_{298}^0 = -13.4 \text{ kJ mol}^{-1}$) is obtained from thermodynamic data [39]. The reaction (4) has been studied in [40] and its progress is illustrated by XRD patterns in Fig. 6. The primary process – the reduction of copper sulphide by iron while copper metal and iron sulphide are formed – is clearly seen, particularly by inspecting the relative intensities of the diffraction lines of Cu and Fe metal. The process is significantly complicated by the existence of several copper sulphide and iron sulphide phases. Already 1 min of milling decreases the relative amount of djurleite $Cu_{1.94}S$ and increased the fraction of chalcocite Cu_2S. After 10 min of milling, only the reflections from Cu, cubic FeS and Fe can be observed. With increasing time of milling cubic FeS changes to its hexagonal modification troilite FeS. This phase is considered the stable modification of stoichiometric FeS [41].

Figure 7 shows the room temperature magnetization data for investigated samples as a function of external magnetic field. It is evident that the resulting magnetization curves are well saturated after an application of magnetic field higher than 2 T. The difference in the saturation magnetization of the samples
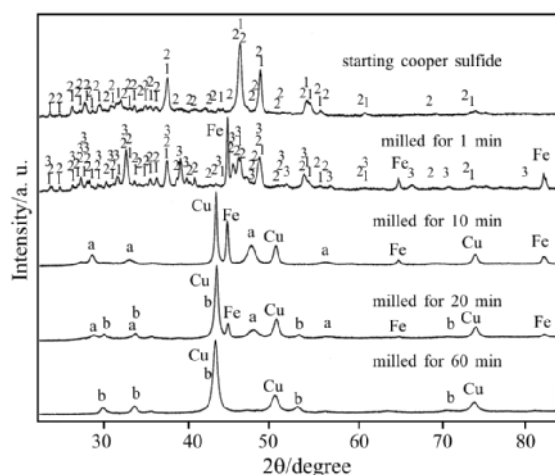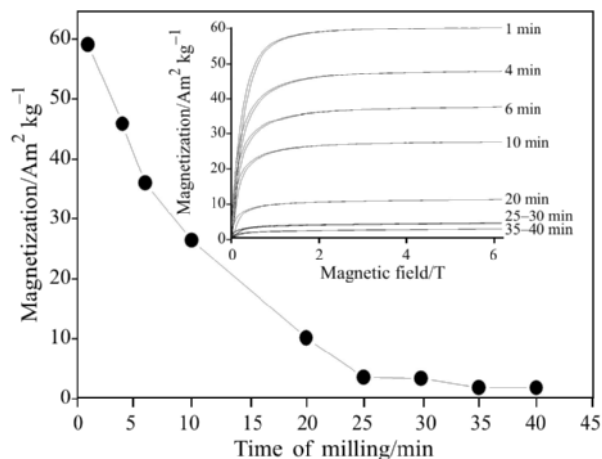

Fig. 7 Magnetization as a function of external magnetic field and/or of milling time for reaction (1) [40]
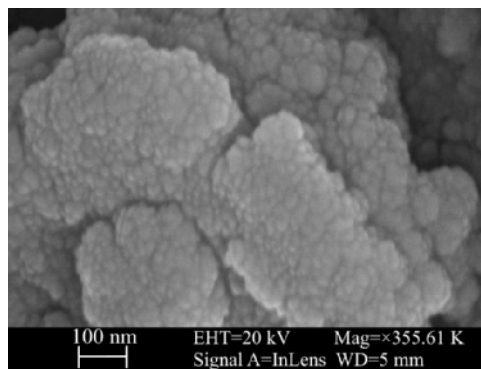

Fig. 8 SEM image of the products of reaction (4)

milled for different times, as displayed in the inset of this figure, is mainly caused by a various amount of the ferromagnetic component in these samples. The inset shows that the amount of metallic iron, which is the only ferromagnetic component in samples, decreases continuously for milling times up to 40 min. At this time the saturation magnetization is negligible indicating that the constituent phases are almost entirely paramagnetic and/or antiferromagnetic, i.e. the reaction (4) tends to be finished.

Surface morphology of the synthesized Cu/FeS nanoparticles with estimated size from 20–30 nm is depicted in Fig. 8. Individual nanoparticles have tendency to form nanoparticle agglomerates during milling process and both entities can be clearly seen.

Lead sulphide, PbS and iron system

The mechanochemical reaction between lead sulphide PbS and elemental iron can be described by the equation

$$PbS + Fe \rightarrow FeS + Pb \qquad (5)$$

Fig. 6 XRD patterns as a function of milling time. The lines of 1 – copper sulphides djurleite, $Cu_{1.94}S$, 2 – chalcocite, Cu_2S and 3 – tetragonal $Cu_{1.81}S$; a – cubic and b – hexagonal FeS and the metals copper (Cu) and iron (Fe) are marked [40]

The reaction is thermodynamically possible at ambient temperature, as the enthalphy change is negative. The value $\Delta H_{298}^0 = -1.3$ kJ mol^{-1} was calculated from the thermodynamic data published in [39].

The course of the mechanochemical reaction between lead sulphide and iron is illustrated by the XRD patterns in Fig. 9. The reaction has been studied in [42]. The XRD pattern is still dominated by the lines characteristic of PbS which illustrates incomplete recovery. The significant line broadening suggests dramating grain size reduction. The lines of the product phases of elemental Pb and pyrrhotite, FeS, as well as residual Fe were also observed.

It is evident in magnetic measurements (Fig. 10) that the magnetization curves are well saturated after the application of a magnetic field higher than 2 T. The difference in the saturation magnetization of the samples as displayed in the inset of this figure, is
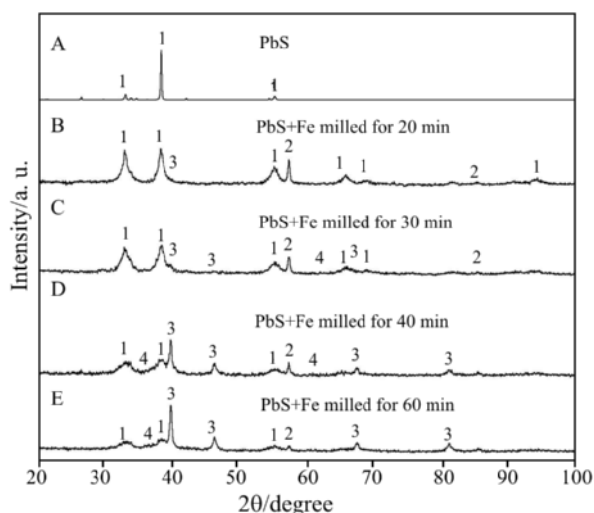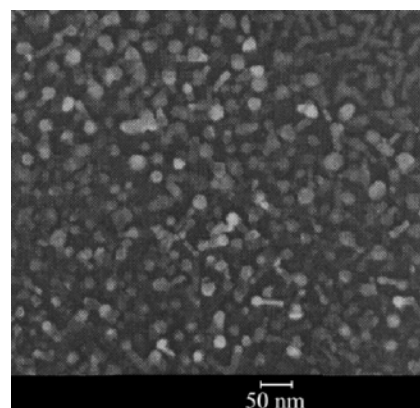

Fig. 11 TEM image of the Pb/FeS nanocomposite prepared by milling for 120 min

mainly caused by the different amount of the ferromagnetic component in the milled samples which is bcc-Fe. For longer milling times the saturation magnetization is negligible indicating that the constituent phases are almost entirely paramagnetic and the mechanochemical reduction is complete.

The reaction product consists of nanocrystalline particles with diameters of 13–21 nm for lead as calculated from XRD line widths. Figure 11 shows a typical TEM image of the mechanochemical product. Examination of TEM shows that the as-milled powder is composed of spherical and rod-like particles. Dimensions of spherical particles are close to the nanometer particle size determined by XRD.

Mechanochemical synthesis of nanocrystalline semiconductors

Nanocrystalline semiconductors have been synthesized by different chemical routes with aim to prepare materials with controlled particle morphology and size distribution [43, 44]. The synthesis routes have used solvothermal synthesis with the addition of microwave, sonochemical and autoclave techniques.

The diverse possibilities of mechanochemical processes for sulphides preparation have been described recently in papers [14–18, 45–53]. In this type of synthesis, chemical reactions and phase transformations of sulphides take place because of the application of mechanical energy. As a consequence, reactions which normally require high temperature will occur at low temperature without any externally applied heat. Mechanochemical processing belongs among the routes which can effectively control and regulate the course of solid-state reactions [54].

A new mechanochemical route for sulphide nanoparticles preparation has been described in [17]. The synthesis is governed by the reaction

$$(CH_3COO)_2M + Na_2S \rightarrow MS + 2CH_3COONa \quad (6)$$

Fig. 9 XRD patterns at different stages of reaction (5) as a function of milling time, A – PbS, B–E – PbS+Fe milled for 20–60 min (1 – lead sulphide, 2 – iron, 3 – lead, 4 – FeS (cubic)) [42]
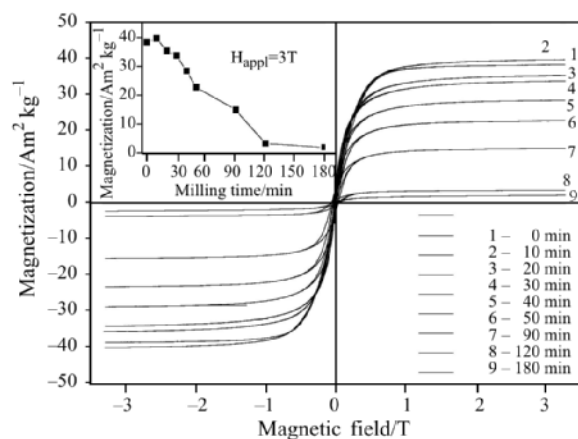

Fig. 10 Magnetization as a function of external magnetic field and/or of milling time for reaction (5) [42]

where *M*=metal and the solid metal nanoparticles MS can be directly obtained by washing the unreacted precursors and soluble product. The synthesis steps are given in Fig. 12.
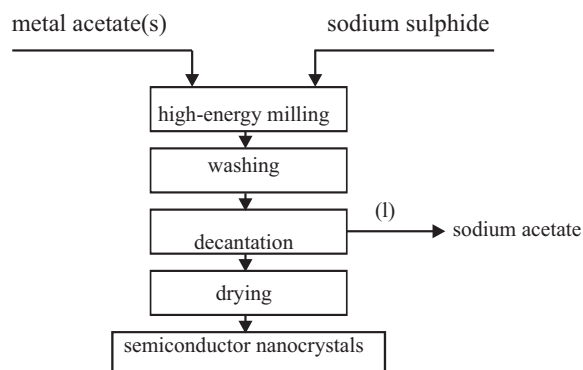

Fig. 12 The synthesis strategy for nanocrystalline semiconductors

Cadmium sulphide

X-ray diffraction pattern of the washed product of the mechanochemical reaction of $(CH_3COO)_2Cd\cdot 2H_2O$ with $Na_2S\cdot 9H_2O$ is given in Fig. 13. Hexagonal α-CdS (G) greenockite (JCPDS 41-1049) together with cubic hawleyite β-CdS (JCPDS 10-454) are present among the products of mechanochemical synthesis. The value of 5 nm was calculated for (111) plane of hawleyite β-CdS (H) nanoparticles. The milling of hexagonal CdS phase brings about its transformation into disordered cubic CdS phase. The rate of this transformation is dependent on the method of preparation of CdS subjected to mechanochemical transformation.
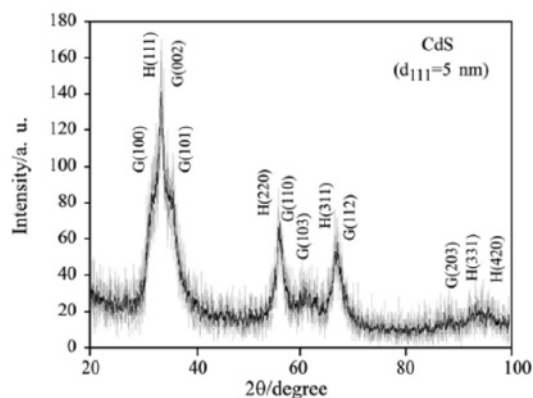

Fig. 13 XRD pattern of the mechanochemically synthesized CdS nanoparticles (JCPDS 6-0313: α-greenockite, JCPDS 10-454: hawleyite β-CdS) [17]

Lead sulphide PbS

XRD pattern of PbS nanoparticles synthesized according to reaction (6) and processed via the flow-

sheet on Fig. 12 is given in Fig. 14. We clearly see the diffraction peaks corresponding to (111), (200), (220), (311) and (222) planes of cubic PbS (galena, JCPDS 5-0592). No other products were confirmed in this well crystallized product with the grain size 8 nm calculated by the Scherrer formula. Surface morphology of the synthesized PbS nanoparticles with the size 20–100 nm is depicted as inset in Fig. 14. Particles form strongly agglomerated entities.

UV-Vis optical absorption spectrum of the mechanochemically synthesized PbS nanoparticles is shown in Fig. 15.

It can be seen that the UV-Vis absorption edge is about 376 nm which correspond to 3.28 eV and shows a blue shift from that the bulk PbS crystals where the direct band gap is 0.41 eV [55]. This is an indication of quantum confinement, because the average size of the PbS nanoparticles is smaller than the excitonic Bohr radius of the bulk PbS (ca. 18 nm) [56].

The mechanochemical synthesis of lead sulphide PbS performed in a laboratory mill and documented by Fig. 14 has been repeated in an industrial mill to verify
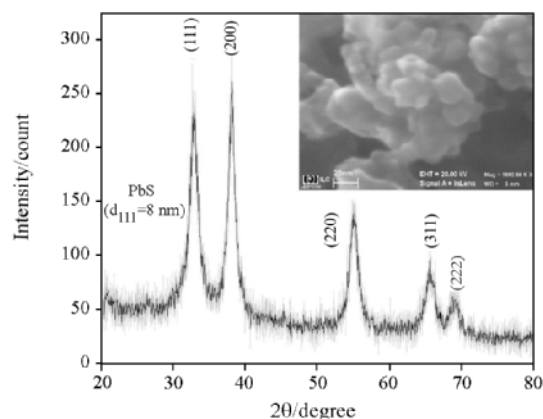

Fig. 14 XRD pattern of the mechanocemically synthesized PbS nanoparticles in a laboratory mill
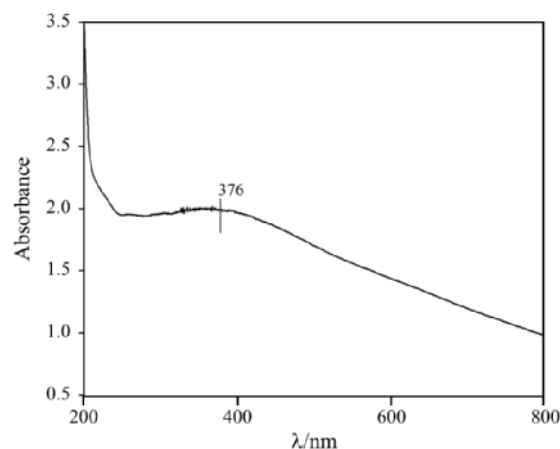

Fig. 15 UV-Vis spectrum of the mechanochemically synthesized PbS nanoparticles
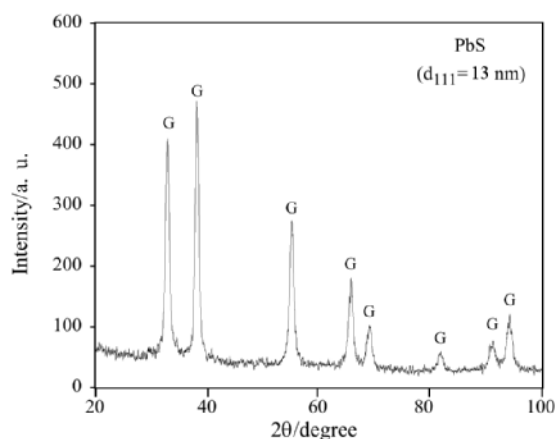
Fig. 16 XRD pattern of the mechanochemically synthesized PbS nanoparticles in an industrial mill, G-galena

the possibility to scale-up the whole process. The obtained PbS nanoparticles have been characterized by X-ray analysis (Fig. 16) and the value 13 nm for the grain size have been calculated. This result indicates the possibility to produce nanocrystalline semiconductors via high-energy milling in an industrial scale.

Conclusions

It is aim of this paper to illustrate some achievements obtained in the mechanochemistry of sulphides in Slovakia. Of course, the presented view is far from complete due to a large international effort in mechanochemistry of sulphides. After successful application to extractive metallurgy of sulphides, mechanochemistry is heading for new fields of study such as nanocrystalline substances and smart materials for the 21st century.

Acknowledgements

References

1 K. Tkáčová, Mechanical Activation of Minerals, Elsevier, Amsterdam 1989.
2 P. Baláž, Extractive Metallurgy of Activated Minerals, Elsevier, Amsterdam 2000.
3 P. Baláž, J. Ficeriová, V. Šepelák and R. Kammel, Hydromet., 43 (1996) 367.
4 J. Ficeriová, Possibilities of Mechanical Activation at Intensification of Non-cyanide Leaching of Gold Bearing Concentrates, Ph.D. Thesis, Institute of Geotechnics, Slovak Academy of Sciences, Košice 2000 (in Slovak).
5 J. Ficeriová, P. Baláž, E. Boldižárová and S. Jeleň, Hydromet., 67 (2002) 37.
6 P. Baláž, J. Ficeriová and C. Villachica, Hydromet., 70 (2003) 113.
7 P. Baláž, R. Kammel and M. Achimovičová, Metall, 48 (1994) 217.
8 P. Baláž, F. Sekula, Š. Jakabský and R. Kammel, Miner. Eng., 8 (1995) 1299.
9 M. Achimovičová, Intensification of Chemical Pretreatment of Sulphidic Minerals, Ph.D. Thesis, Institute of Geotechnics, Slovak Academy of Sciences, Košice 1998 (in Slovak).
10 P. Baláž, M. Achimovičová, J. Ficeriová, R. Kammel and V. Šepelák, Hydromet., 47 (1998) 297.
11 P. Baláž, Mater. Sci. Forum, 312–314 (1999) 215.
12 P. Baláž, Metall, 54 (2000) 190.
13 E. Godočíková, Chloride Leaching of Mechanically Activated Complex CuPbZn Concentrate, Ph.D. Thesis, Institute of Geotechnics, Slovak Academy of Sciences, Košice 2001 (in Slovak).
14 P. Baláž, Z. Bastl, T. Havlík, J. Lipka and I. Tóth, Mater. Sci. Forum, 235–238 (1997) 217.
15 P. Baláž, L. Takacs, T. Ohtani, D. E. Mack, E. Boldižárová, V. Soika and M. Achimovičová, J. Alloys Compd., 337 (2002) 76.
16 P. Baláž, L. Takacs, J. Z. Jiang, V. Soika and M. Luxová, Mater. Sci. Forum, 386–388 (2002) 257.
17 P. Baláž, E. Boldižárová, E. Godočíková and J. Briančin, Mater. Lett., 57 (2003) 1585.
18 P. Baláž, L. Takacs, E. Boldižárová and E. Godočíková, J. Phys. Chem. Solids, 64 (2003) 1413.
19 V. V. Lodejščikov and I. D. Ignateva, Processing of Silver Bearing Ores, Nedra, Moscow 1973 (in Russian).
20 I. J. Corrans and J. E. Angove, Miner. Eng., 4 (1991) 763.
21 G. Heinicke, Tribochemistry, Akademie – Verlag, Berlin 1984.
22 V. G. Gould, Eng. Min. J., 156 (1955) 91.
23 H. Gleiter, Progr. Mater. Sci., 33 (1989) 223.
24 H. Gleiter, Nanostruct. Mater., 1 (1992) 1.
25 H. Gleiter, Nanostruct. Mater., 6 (1995) 3.
26 H. Gleiter, Acta Mater., 48 (2000) 1.
27 C. Suryanarayana, Int. Mater. Rev., 40 (1995) 41.
28 B. S. Murty and S. Ranganathan, Int. Mater. Rev., 43 (1998) 101.
29 J. S. Benjamin, Metall. Trans., 1 (1970) 2946.
30 J. S. Benjamin, Sci. Am., 234 (1976) 40.
31 C. C. Koch, Nanostruct. Mater., 2 (1993) 109.
32 A. R. Yavari, Mater. Trans. JIM, 36 (1995) 228.
33 P. G. McCormick, Mater. Trans. JIM, 36 (1995) 161.
34 C. C. Koch, Nanostruct. Mater., 9 (1997) 13.
35 E. Gaffet, F. Bernard, J.-C. Niepce, F. Charlot, Ch. Gras, G. Le Caër, J.-L. Guichard, P. Delcroix, A. Mocellin and O. Tillement, J. Mater. Chem., 9 (1999) 305.
36 C. Suryanarayana, Progr. Mater. Sci., 46 (2001) 1.
37 C. Suryanarayana, E. Ivanov and V. V. Boldyrev, Mater. Sci. Eng. A, 304–306 (2001) 151.
38 L. Takacs, Progr. Mater. Sci., 47 (2002) 355.
39 O. Kubaschewski and L. L. Evans, Metallurgical Thermochemistry, Pergamon Press, London 1995.
40 P. Baláž, L. Takacs, J. Z. Jiang, V. Soika and M. Luxová, Mater. Sci. Forum, 386–388 (2002) 257.
41 P. Baláž, E. Godočíková, Z. Bastl, J. Z. Jiang, E. Boldižárová and M. Luxová, Czech. J. Phys., 52 (2002) A65.

42 E. Godočíková, P. Baláž, E. Boldižárová, I. Škorvánek, J. Kováč and W. Choi, J. Mater. Sci., 39 (2004) 5353.

43 R. Houbertz, W. Krauss, R. Birringer and U. Hartmann, Nanostruct. Mater., 9 (1997) 339.

44 S. H. Yu Wu, J. Yang, Z. H. Han, Y. Xie, Y. T. Qian and X. M. Lin, Chem. Mater., 10 (1998) 2309.

45 L. Takacs and M. A. Susol, J. Solid State Chem., 121 (1996) 394.

46 L. Takacs, Mater. Sci. Forum, 269–272 (1998) 513.

47 T. Ohtani, K. Maruyama and K. Ohsima, Mater. Res. Bull., 32 (1997) 343.

48 T. Ohtani, A. Tsubota and K. Ohsima, Mater. Res. Bull., 34 (1999) 1143.

49 T. Tsuzuki and P. G. McCormick, Appl. Phys., A65 (1997) 607.

50 T. Tsuzuki and P. G. McCormick, Nanostruct. Mater., 12 (1999) 75.

51 R. Lin, J. Z. Jiang, R. K. Larsen, S. Morup and F. J. Berry, Hyperfine Interact. C, 3 (1998) 45.

52 J. Z. Jiang, R. K. Larsen, R. Lin, S. Morup, K. Chorkendorff, K. Nielsen, K. Hansen and K. West, J. Solid State Chem., 138 (1998) 114.

53 F. Saito, Q. Zhang and J. Kano, J. Mater. Sci., 39 (2004) 5051.

54 V. V. Boldyrev, Russ. Chem. Rev., 75 (2006) 177.

55 M. T. Nenadovice, M. I. Comor, V. Vasic and O. I. Micie, J. Phys. Chem., 94 (1990) 6390.

56 W. Wang, Y. Liu, Y. Zhan, Ch. Zheng and G. Wang, Mater. Res. Bull., 36 (2001) 1977.